中國機械工程學刊第四十一卷第二期第 211~220 頁(民國一百零九年)
Journal of the Chinese Society of Mechanical Engineers, Vol.41, No.2, pp 211~220 (2020)

Upgrade of The Wind Turbine Pitch Driving System for High-Turbulent Wind Operation

Jui-Hung Liu*, Jien-Chen Chen **, Chin-Cheng Huang*** and Wen-Jeng Lai***

Keywords： wind turbine, blade pitch system, turbulent intensity, O&M, pitch motor.

ABSTRACT

Wind speed and wind direction received much attention during the WTG (wind turbine generator) operation. However, the WTG operation is highly determined by the turbulence intensity (T.I.) as well. Malfunctions of the WTG could have been taken place even the wind speed and the wind T.I. are within the WTG operation specification. This work is a case study of the influence of wind T.I. on the WTG operation. The research objects are 21 WTGs (Zephyros, model type: Z72, rated power 2000 kW) in mid-Taiwan. Emergency WTG shutdown has been engaged frequently in this wind farm due to the insufficient motor capability for the pitching motion against rapid wind variations. An upgrade of the pitch driving components has been conducted. The capability requirement of the pitching system has been firstly evaluated by software DNV-GL Bladed. Before the practical components' replacement, the performance of new pitch driving module has been investigated with the aid of software DNV-GL Bladed, Adams and Matlab. The efficacy of the improved blade pitching system has been verified by practical operations of three WTGs. The information revealed in this work may be valuable for the future design of pitch regulation system or the operation and maintenance (O&M) for the current WTGs.

INTRODUCTION

The power production (power curve) is an important performance index for wind turbine generators (WTGs). According to the international standard IEC 61400-12-1, the power production of a WTG is mainly determined by the mean wind speed and the air density. However, many studies have shown that WTG power production depends on several variables, and especially the turbulence intensity (T.I.) (Hedevang, 2014). The relationship between power production, wind T.I. and wind speed has been investigated (Lubitz, 2014). At low wind speed, increased turbulence appeared to increase energy production, but power production reduced at high wind speed. Wind T.I. is also crucial for fatigue load and structural design of WTGs (Wang, 2013). Another factor greatly affects the WTG performance is the blade pitch angle. A variable blade pitch system which can turn the blade pitch angle to a degree normally ranges from 0 ~ 90 degree is very important in the modern WTG. The coefficient of power (C_p), which means the wind energy conversion efficiency of the WT blade, is greatly dominated by the blade pitch angle. The pitch angle is the angle between the blade and the blades rotation plane. The attack angle is the angle between the chord of the aerofoil and the relative wind, as shown in Figure 1(Horizon, 2012).

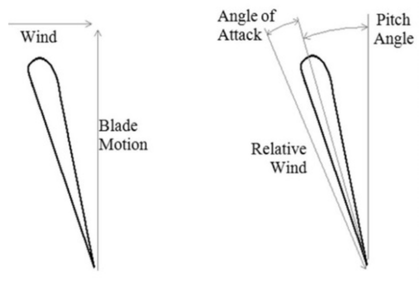

Fig 1. Definition of pitch angle and angle of attack (Horizon, 2012)

$$T.S.R. = \lambda = \frac{wr}{V}\text{, } w\text{ :rotational speed, } r\text{: radius at the specified point, } V\text{: wind speed.} \quad (1)$$

The angle of attack is dependent on blade twist and

Paper Received May, 2019. Revised June, 2019, Accepted July, 2019, Author for Correspondence: Jui-Hung Liu.

* *Southern Taiwan University of Science and Technology, Department of Mechanical Engineering, Tainan, Taiwan, 701.*

** *Industrial Technology Research Institute, Green Energy and Environment Research Laboratories, Hsinchu, Taiwan, 304.*

*** *Institute of Nuclear Energy Research, Taoyuan, Taiwan, 411.*

pitch. For most aerofoils, lift force can be maximized at an attack angle between 10 and 15 degrees. A parameter in the WTG performance analysis is the tip speed ratio (TSR) which is defined as the linear speed of the blade tip divided by the prevailing wind speed(V) as shown in Equation 1. For a given wind speed, a lower pitch angle will result in a higher TSR at the maximum lift. A larger pitch angle will tend to give the maximum lift, and thus greater torque, at a lower TSR. Higher C_p can be achieved by blades with lower pitch angles and higher TSR. The schematic diagram of the aerofoil section and the forces acting on it are shown in Fig 2 (Sudhamshu, 2016). The plane of the blade rotation is depicted as a line in the figure. With respect to the blade rotation plane, the chord line is given a twist called the section twist angle β. This angle varies along the length of the blade for the reason to maintain a constant attack angle along the blade length. For dynamic control of the blade, an additional twist called global pitch angle ϕ can be applied. This pitch angle would change as the twist varies at every cross section. The resultant force on the blade due to the flow around the blade may be resolved in two ways: (1) along the incoming velocity – Normal force (F_N) and along the plane of rotation – Tangential Force (F_T); (2) along the direction of the relative velocity – Drag force (F_D) and the other perpendicular to the relative velocity – Lift force (F_L). These forces may be related as follows:

$$F_N = F_L \cos\theta + F_D \sin\theta, \tag{2}$$
$$F_T = F_L \sin\theta - F_D \cos\theta. \tag{3}$$

Coefficient of normal and tangential force is the nondimensionalized form of F_N and F_T given by Eq. (4).

$$C_{N,T}=F_{N,T} / 0.5\rho[V_{in}^2+(r\omega)^2]. \tag{4}$$

The pressure distribution across the aerofoil may be quantified by the coefficient of pressure (C_{pre}) defined as

$$C_{pre} = (p-p_\infty) / 0.5\rho[V_{in}^2+(r\omega)^2]. \tag{5}$$

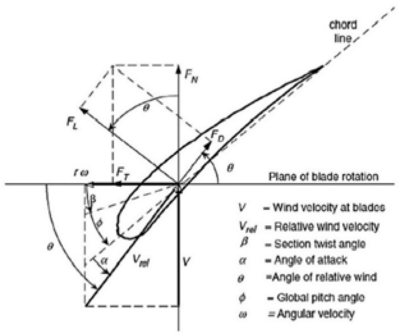

Fig 2. Forces on an aerofoil (Sudhamshu, 2016)

Considering a three-bladed, horizontal-axis, pitch-controlled WTG, as illustrated in Fig 3 (B. Biegel, 2011). The y-and z-axes span the rotor plane while the x-axis is perpendicular to the rotor plane. In the assumption that the WTG is under the influence of a wind field that is constant over time but varying over the area swept by the blades. The blades are numbered in 1, 2, 3 and the angle $\gamma \in [0, 2\pi/3]$ is referred to the rotor position. Since the wind flow is assumed to be constant over time, the blade pitching is a periodic function of the angle γ. The pitching angles of three blades at angle γ can be expressed as follows:

$$\phi(\gamma) = (\phi_1, \phi_2, \phi_3) \in R^3 ,\ 0 \le \gamma \le 2\pi/3 \tag{6}$$

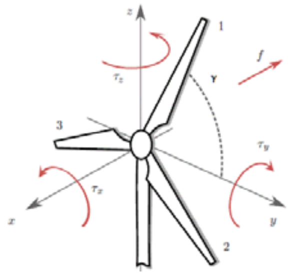

Fig 3. Overview of a wind turbine (Biegel, 2011)

The generated torques around the three main axes, $\tau = (\tau_x, \tau_y, \tau_z) \in R_3$, are determined by these pitch angles and a net force f, is finally acted on the WTG structure. The induced torques (τ) and the resulted force (f) depend on the angle of the rotor, the pitch of the blades, the wind field present at the swept area and the angular velocity of the rotor. If a constant rotor angular velocity is given and the wind field at the swept area is defined by a parameter vector η, the induced torques and the resulted force (f) can be further expressed as follows (Biegel, 2011):

$$\tau = \Psi(\phi(\gamma), \gamma, \eta), f = Y(\phi(\gamma), \gamma, \eta). \tag{7}$$

The aerodynamic loads are usually resolved into thrust (T) in the direction of rotation absorbed by the generator and reaction forces (R), as shown in Fig 4 (Schubel, 2012). It can be observed that the reaction force is substantially acting on the flatwise bending plane and must be tolerated by the blade with limited deformation.

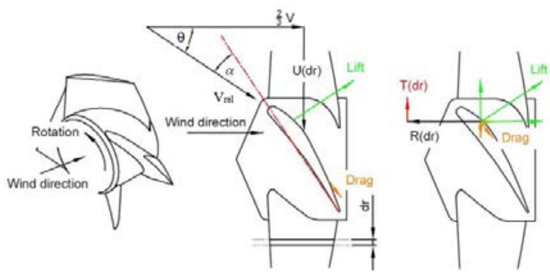

Fig 4. Forces at a blade element (Schubel, 2012)

Despite the rapidly growing wind farm installations worldwide, atmospheric and wake turbulence interactions are not well understood with respect to the fatigue loads on wind turbines (Lee, 2013). Though turbulence in the approaching wind has a significant impact on the power output of WTGs (Hedevang, 2014 & Wang, 2013), more attentions have been devoted to the damages induced by turbulence. The WTG response to turbulent inflow has been studied by NREL (National Renewable Energy Laboratory, America) (Hand, 2003). The turbulence causes increased fatigue loads on WTG blades and it can be generated above the surface layer under some atmospheric conditions. The atmospheric conditions supporting turbulence production through dynamic instabilities occur during a significant percentage of the WTG operation regime. A computer program was accomplished to determine the blade-root fatigue damage (Noda, 1999). The effects of T.I., mean wind speed, wind shear, vertical wind component, dynamic stall, stall hysteresis and blade stiffness were all examined in that work. An advanced turbulence model was proposed to evaluate the relationship of T.I. and wind speed for fatigue load estimation and WTG structural design (Wang, 2013). Similar analyses of blade fatigue life regarding the influence of tower shadow (Pedersen, 2012) and wind speed distribution (Jang, 2015) were also reported respectively.

Most of the past researches are mainly focused on the structural considerations of WTGs. However, the dynamic loading also exerted on the components inside the nacelle, such as the gearbox, the generator, motors and hydraulic actuators. The influence of wind turbulence on yaw-control gears was studied (Suzuki, 2011). According to the practical measurements, high turbulence may result in an oscillating torque, which is greater than the metal fatigue limit, to yaw-control gears. The wind turbine control system has a large effect on many operation conditions. For instance, during normal operation, collective blade pitch control can be used to reduce the fatigue loads on the tower, individual pitch control can reduce the fatigue loading on the blades, and generator torque control can reduce fatigue loading on the drive train (E. Bossanyi, 2010)-(Kanev and Engelen, 2009). A pitch control technique has been reported against high wind gusts (Nanayakkara, 1996). The pitch system frequency and WTG power output are regulated according to the wind speed and the wind turbulence. Since WTG system is a high-order nonlinear system, a pitch control method based on the active-disturbance-rejection control theory has been proposed to improve the shortcoming of conventional PI controller (Xia, 2014). Linear models of the WTG and the drive train have been derived to improve the control performance under strong wind turbulence. A control strategy was introduced for reduction of extreme loads on WTG components during operation in extreme turbulence conditions (Kanev, 2016 & Kanev, 2017). The control algorithm is based on estimation of the wind turbulence, followed by reduction of the rated rotor speed whenever this turbulence estimate exceeds certain limit. An optimization approach has been developed to calculate the turbulence limit so as to achieve the best balance between alertness and false alarms. For the purpose to regulate the generator speed and to mitigate the induced load under turbulent wind field, an adaptive pitch control strategy has been formulated (Yuan, 2017). The control algorithm makes a trade-off between the maximum energy captured and the load induced. The simulation results show that the blade root flapwise load can be reduced at a slight expense of optimal power output.

The researches regarding the pitch control system are mainly focused on the system operation mode, for instance, the frequency, the limit and the speed for the pitching action. However, once the hardware specification of pitch control system is insufficient against the wind field (means the operational capability of the WTG is not sufficient against the local wind conditions and leads to a shutdown frequently), an emergency shutdown (trip) is going to be engaged and the operation mode will no longer be conducted. In other words, the efficiency of wind power harvest will be completely unqualified if the WTG trip is met of high frequency. An investigation regarding the wind turbulence influence on the WTG pitching system has been revealed in this work. Namely, the study of pitch control system specifications against aerodynamic loads. The research object is a wind farm in mid-Taiwan. Totally 21 WTGs installed in this wind farm (WTG model: Zephyros Z72, rated power 2000 kW). The root cause of WTG trips (shutdown) has been investigated according to actual recordings of the WTG operation and the wind condition. The software DNV-GL Bladed, Adams and Matlab have been employed for the analyses of WTG subsystem capability requirements and performance verifications. An upgrade of pitch motors and the corresponding drivers has been finally applied to these WTGs to improve the problems of the WTG overspeed and the pitch motor overcurrent and to mitigate the fatigue load on the turbine structure simultaneously.

WTG malfunctions due to high-turbulent wind flow

Taiwan is located between Asia and Pacific. This island is suffered from north-eastern monsoon in winter and spring, while southwestern monsoon in summer and autumn. According to the 10-year global wind speed rankings from Jan. 2000 to Dec.

2009 (4C Offshore, 2017), the top 30 wind farms are almost located in the surroundings of Taiwan Strait. Since the north-eastern monsoon in Taiwan is generally much stronger and more copious than southwestern monsoon, wind energy harvest is mainly engaged during the end and the beginning of a year. WTGs installed in Taiwan are mainly purchased from manufacturers in Europe or U.S. Though all these WTGs are fulfilled with the standards of IEC or GL, malfunctions still met frequently due to the climatic variations and geographic nature of Taiwan. Normally, the average operation availability of a well-operated wind farm should be higher than 95% in global onshore wind market. However, WTG operation availability of Taiwan, as shown in Fig 5 (Taipower Company, 2017), is about 92% in 2013, still below the global average. The unique wind condition of Taiwan is conducive to the expansion of wind energy industry, the climatic particularity also leads to an unqualified operation availability. The research object of this work is the Z72 WTG, which is manufactured by Zephyros. The technical specifications of Z72 are listed in Table 1.

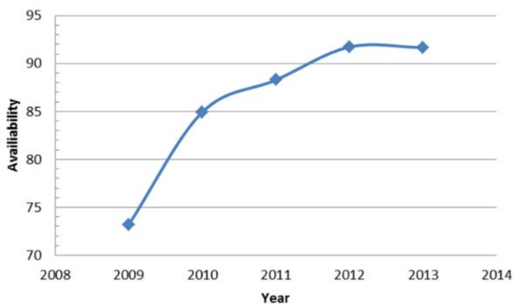

Fig 5. Operation availability of WTG in Taiwan

Table 1. Technical Specifications of Zephyros Z72 WTG (Moerman, 2009)

Specifications	Descriptions
Rotor diameter	70.65 m
Rotor speed	Variable, nominal 22.5 rpm
Nominal power	2000 kW
Transmission	Direct drive generator, single main bearing
Rated wind speed	12.3 m/s
Cut-in / Cut-out Wind speed	3-25 m/s
Survival wind speed	70 m/s
Rotor speed control	Blade pitch
Wind class	2 and S according to IEC 61400-1
Generator mass	49 tons
Rotor mass	36 tons
Nacelle mass	12 tons

There are totally 21 Z72 WTGs installed in the mid-western coast of Taiwan, the location is illustrated in Fig 6 (Taiwan Power Company, 2017). According to the technical document of Z72 (Table 1 (Moerman, 2009)) and the IEC standard (Table 2 (IEC, 1999)), Z72 is designed to operate under the class IB wind condition. That is, Z72 can be operated under a yearly average wind speed beyond 10m/s and the T.I. below 0.16. The T.I. is calculated by σ/V_{hub}, where σ is the standard deviation of the wind speed during a specified period and V_{hub} is the average wind speed at hub height.

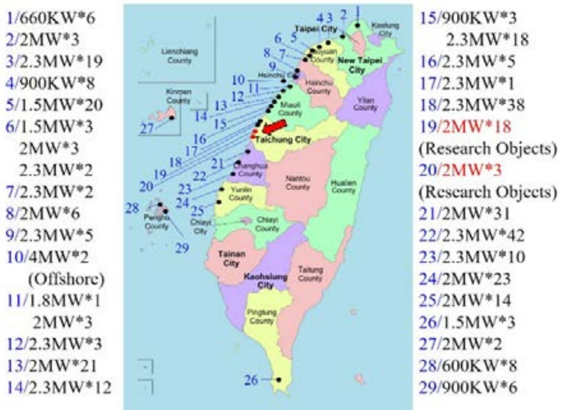

Fig 6. Research objects: Z72 WTGs in Mid-Taiwan

Table 2. IEC standards for WTG classes (IEC 61400-1 2nd edition) (IEC, 1999)

Wind turbine class	I	II	III	S
V_{ref} (m/s)	50	42.5	37.5	Values specified by the designer
V_{avg} (m/s)	10	8.5	7.5	
A I_{ref} (-) (T.I.)		0.18		
B I_{ref} (-) (T.I.)		0.16		

However, more than 30 times of WTG overspeed or pitch motor overcurrent events were triggered for an individual WTG during the period of north-eastern monsoon (from Oct. 2013 to Mar. 2014). These kinds of trip events brought excess fatigue damage to the structure and cut down a lot of power production as well. The variations of wind speed and wind T.I. during the period of north-eastern monsoon are exhibited in Fig 7 and Fig 8. Though the average wind speed during this period is merely 6.2m/s, while the average T.I. is calculated to be 0.17. The T.I. is a bit higher than that of class B in Table 2. The average T.I. measured for individual WTGs on another day is listed in Table 3. It can be observed that the turbulence intensities belong to WTGs #P02, #P03, and #H18 are much higher than those of the other 17 WTGs. Though the average T.I. in a day is not as high as the index I_{ref} defined in Table 2., the instantaneously extreme T.I. leads to the WTG overspeed and may be clarified based on the WTG speed recording on Oct. 04, 2013. An overspeed recording for WTG #P03 is exhibited in Table 4. Before the overspeed taken place, the pitch angle is regulated along with the wind speed to maintain the required power output. However, a reverse variation of wind speed occurred around 18:36. The wind speed is suddenly much increased and leads to a rotor overspeed (threshold 26.5 rpm). The T.I. for this very short period is about 22.82% (beyond the IEC standards). The interaction between wind speed, rotor speed, and pitch angle can be clearly interpreted by Fig 9. The system response of pitch regulation is not capable of slowing down the rotor against extreme turbulent wind. It also means the torque output of pitch motor is insufficient to restrain the induced wind force.

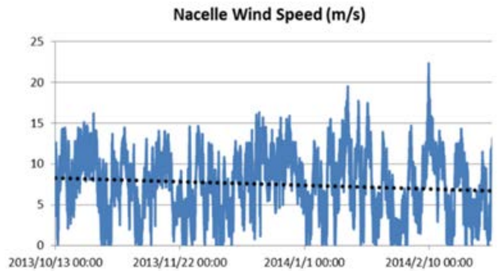

Fig 7. Wind speed of Z72-WTG wind farm during the period of north-eastern monsoon

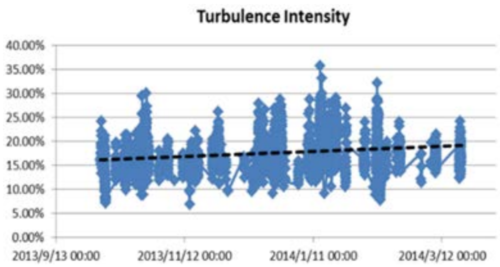

Fig 8. Wind turbulence intensity of Z72-WTG wind farm during the period of north-eastern monsoon

Table 3. Average turbulence intensity (T.I.) on Oct. 04, 2013

WTG No.#	T.I.	WTG No.#	T.I.
P02	0.153	H09	0.075
P03	0.156	H10	0.062
P04	0.112	H11	0.074
H01	0.072	H12	0.067
H02	0.849	H13	0.066
H03	0.061	H14	0.071
H04	0.093	H15	---
H05	0.070	H16	0.074
H06	0.078	H17	0.086
H07	0.078	H18	0.141
H08	0.082	---	---

Remark: WTG #H15 was under maintenance

Table 4. Overspeed recording of WTG #P03

Time (min.: sec.)	RPM	Wind Speed (m/s)	Pitch Angle (deg.)
18:20	22.1	16.01	12.2
18:25	21.6	13.14	8.1
18:31	21.5	10.85	2.92
18:36	**30.2**	17.02	10.4
18:41	8.3	14.04	50.8

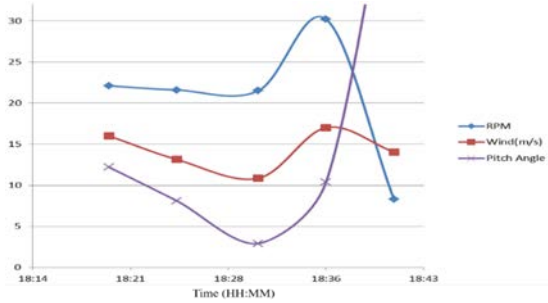

Fig 9. Interaction between rotor speed, wind speed and pitch angle

Improvements on pitch regulation system

Analysis of original pitch regulation system

An investigation for the original pitch regulation system has been performed to find out the root cause of the WTG trip. Fig 10 (Harakosan, 2013) is an overview of the original pitch system in the hub of a Z72 WTG. The pitch control box is equipped in the hub to issue the command for the three blades. Each blade is driven by an exclusive pitch motor, as shown in the bottom of Fig 10. A detail blade pitch driving module is depicted in Fig 11. The gear ratio of the planetary gearbox is 1: 280 and the total gear ratio is 1: 2380. Namely, the pitch bearing torque should less than 2380*11 Nm = 26.18 kNm during WTG operation, where the number 11 is the rated torque output of the original pitch motor.

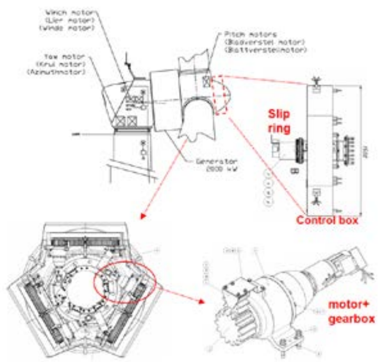

Fig 1. Pitch system overview for the Z72 wind turbine

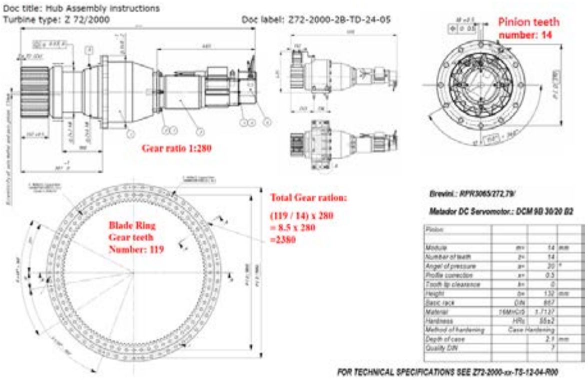

Fig 11. Pitch motor and its gear assembly

The required motor torque output against the high-turbulent wind like those in Table 3 can be evaluated by the software DNV-GL Bladed (DNV-GL, 2011). In the consideration of design load case (DLC) 1.2 of IEC 61400-1 design guideline (IEC, 2010), blade pitch bearing loads under turbulent wind conditions have been estimated by DNV-GL Bladed and illustrated in Fig 12. The statistics for Fig 12 have been listed in Table 5. At rated wind speed 12m/s, the blade pitch bearing has the highest average load (19.92 kNm) because the pitch angle ϕ is set to zero to absorb the maximum power from the wind. For other wind speed conditions higher than 12m/s, the pitch bearing moments are lower due to the load mitigation effect by the blade pitching. It is obviously that the resulted pitch bearing load can easily exceeds the torque output limit (26.18 kNm) of the original pitching system. The rated torque output of the original driving module is 11 Nm and the brake torque is 16 Nm. Once the blade encounters such kind of wind conditions, the overcurrent will certainly be triggered, and the controller will shut down the WTG immediately. For example, a load of 15 Nm applied to the motor and the resulted motor current will be 15/0.55(torque constant) = 27.27 A. That means the malfunctions of Z72 WTGs are due to the insufficient power of pitch control actuator.

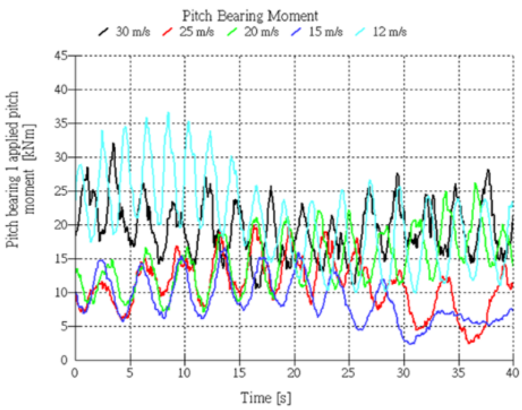

Fig 12. Load of blade pitch bearing under various wind conditions

Table 5. Pitch bearing moment analysis (Units: kNM)

m/s	Min	Mean	Max	Std. Dev.
30	9.24638	18.9638	32.103	4.20775
25	2.4456	10.8992	19.9525	3.85956
20	5.63691	13.9513	26.2141	4.25027
15	2.24972	11.551	40.4894	7.70106
12	9.86087	19.92	36.6597	6.21865

Verification of upgraded pitch regulation system

According to the analysis results shown in Fig 12, a new pitch driving module should be employed to replace the original components. The new driving motor should fit in with the controller operation requirements, the installation space, the connection interface between the motor and the original planetary gearbox and do not affect the WTG stiffness anymore. The comparison of the original module and the employed new module are listed in Table 6. The improvement includes 50%, 20%, 160% and 50% increase in the motor rated current, the motor rated torque, and the motor rated power and the maximum transient current of motor driver respectively

Table 6. Comparison between original and new blade pitch regulation driving module

Specifications	Original	Required
Motor Rated voltage (VCD)/ current (A)	171 / 20	160 / 30
Motor Rated speed (RPM)/ torque (Nm)	3000 / 11	3000 / 13
Motor Rated power / Max power (kW)	1.5 / 3.4	3.9 / 4.8
Motor Brake torque (Nm)	16	32
Drive power (kW)/ Max transient current (A)	5 / 35	5 / 52
Inductive (mH)	2.3	1.3
Resistence (ohm)	0.31	0.31
K_i (Nm/A) Torque Constant	0.55	0.433
K_w V/(rad/s) Voltage Constant	0.55	0.50
Motor Inertia (Kg-m^2)	0.01	0.01

Before the practical components' replacement, the performance of new pitch driving module has been investigated with the aid of software DNV-GL Bladed, Adams and Matlab. The actual wind condition data of Z72 wind farm is also employed in these analyses. The analysis flowchart is illustrated in Fig 13. DNV-GL Bladed is employed to evaluate the loading for blade pitch bearing and Adams is for the analysis of WTG dynamics. The wind conditions, the pitching loads and the system dynamics will be all included in the pitching motion analysis by Matlab. The analysis results under wind speed from 10 m/s to 18 m/s and 15 m/s to 25 m/s are shown in Fig 14 and Fig 15 respectively. Fig 14 is the medium wind speed case. The average wind speed is 13.6 m/s and the average motor current is 3.98 A. The resulted max blade torque load is 19 kNm and the instantaneous motor torque load is 12 Nm. In Fig 15, the average wind speed is 18.1 m/s and the average motor current is 5.37 A. Although the max instantaneous motor torque load is up to 19 Nm, the overload case will not occur due to the new motor driver. The new driving module can provide two times of rated torque output in 3 seconds (the rated torque output is 13 Nm). Both the simulation results have shown a qualified performance of the new pitch regulation system. As a result, new driving modules have been practically applied to the WTGs #P02~#P04 for a preliminary validation, as shown in Fig 16 and Fig 17. Fig 17(a) is the pitch motor driver within the WTG hub. The components of a motor driver can be seen in Fig 17(b), which includes a DC motor driver, a power supply and an Emergency Control Module (ECM).

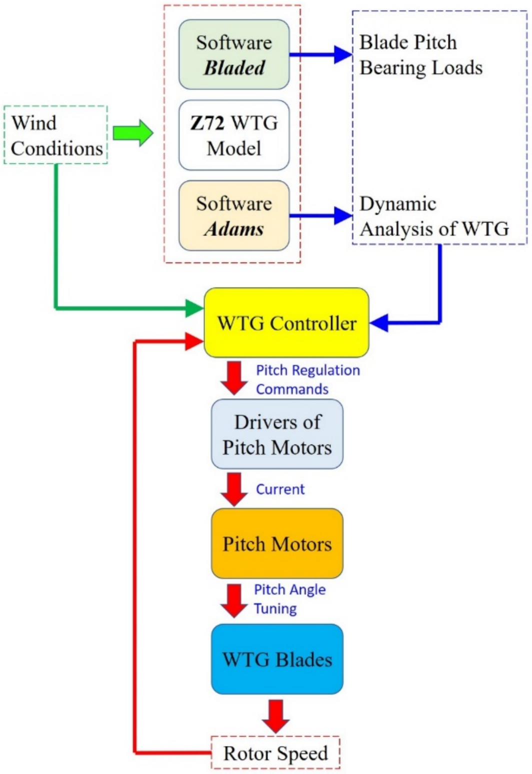

Fig 2. Flowchart of analysis for pitching system

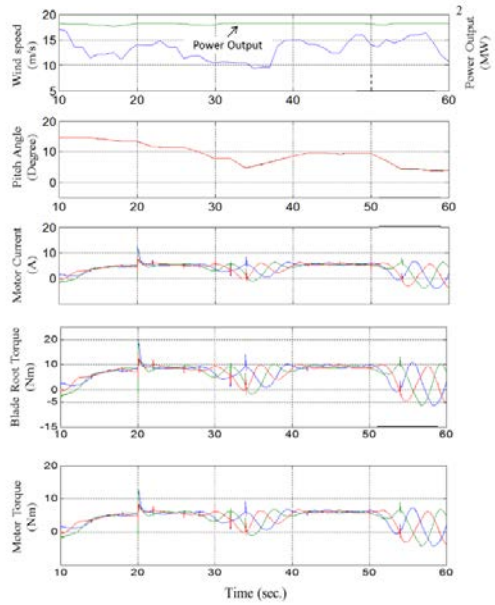

Fig 14. System response of pitch regulation under wind speed from 10m/s to 18m/s

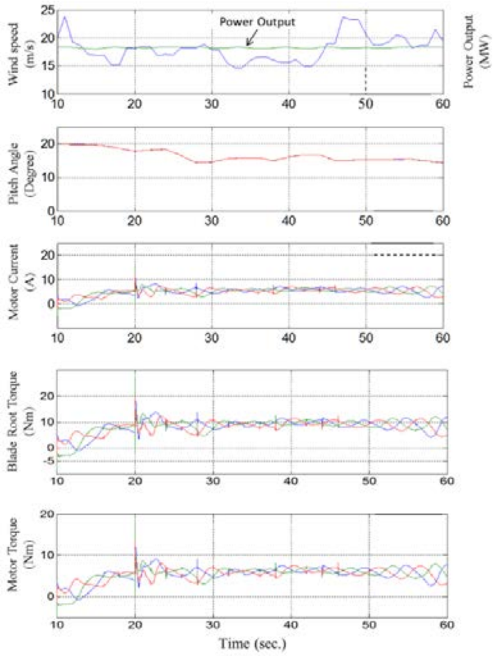

Fig 15. System response of pitch regulation under wind speed from 15m/s to 25m/s

Fig 16. Pitch motor: old motor(left)/new motor(right)

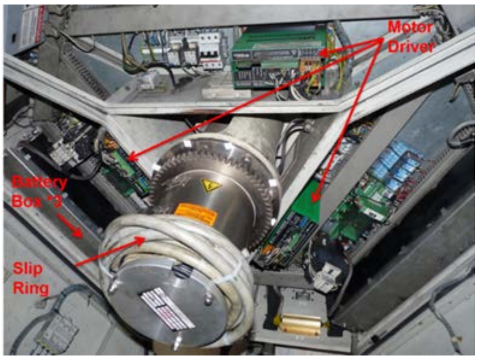

(a)

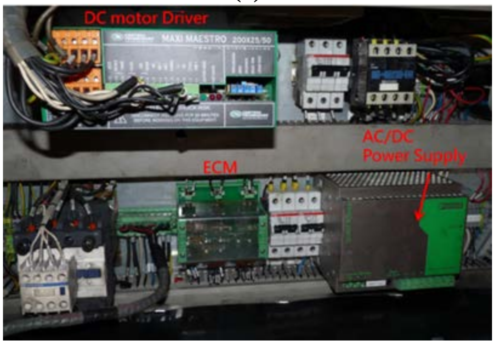

(b)

Fig 17. Upgraded pitch motor driver

Regulation performance of improved pitch control system

Practical performance of new pitch control system for WTG #P03 has been demonstrated in Fig 18~Fig 20. The average wind speed for Fig 18 is 13.4m/s (slightly exceeds the rated wind speed of Z72). Under this wind condition, the average motor current is 4.69A while an instantaneous peak of 24.8A has been observed. Both original system and new system can operate well under this situation. The second case is referred to Fig 19; the wind condition is measured at 22nd July 2014. The average wind speed and the instantaneous peak wind speed are 22.5 m/s and 35 m/s respectively. For this case, the induced average motor current is 5.3A with an instantaneous peak of 28.1 A. The new pitch control system still operates well under this wind condition, but a trip may be triggered for the original system due to the rated motor current limit (see Table 6). Finally, the last illustration is a severe wind speed case. The wind condition in Fig 20 is also measured at 22nd July 2014 and the average wind speed is beyond 25 m/s. A sudden increase of wind speed has been observed around 50 sec. The three blades therefore should be pitched from the working angle (0 degrees) to the idling angle (84 degrees) to protect the WTG, as shown in Fig 20. Since the max transient current of new system is up to 52A (least for three seconds), the blades can pitch off continuously even the motor current exceeds the rated specification (see Table 6 and Fig 20). The practical performance of the updated system (variations of motor parameters) is fit in with the analysis results of Sec. 3. The practical wind conditions (shown in Fig 18 ~ Fig 20) for the WTG #P03 is comparable to those recorded on Oct. 04, 2013 (Listed in Table 3 and Table 4). Namely, both the driving motor specification and the pitching motion have been confirmed to be qualified for the local wind conditions.

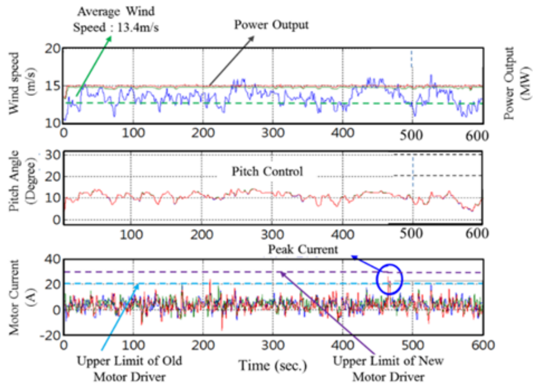

Fig 18. WTG performance under normal wind speed (Average wind speed: 13.4 m/s)

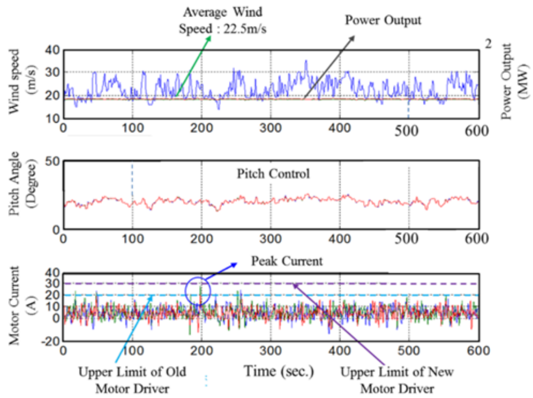

Fig 19. WTG performance under high wind speed (Average wind speed: 22.5m/s)

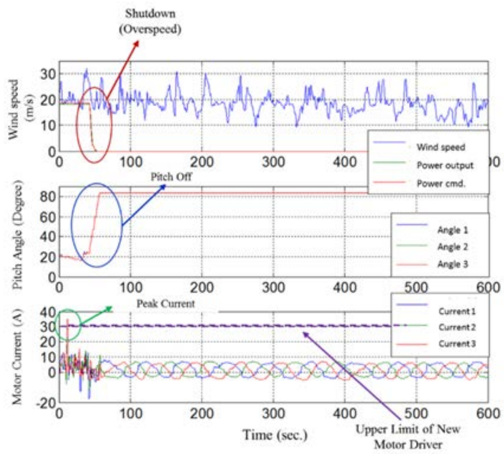

Fig 20. WTG performance under severe wind speed

Conclusions

The operation of 21 WTGs in the mid-western coast of Taiwan has been investigated in this work. According to the local wind recordings, the instantaneous turbulence intensity of this wind farm is quite high and leads to high frequency trip events. An upgrade of pitch driving system has been proposed in this work. The system requirements are evaluated by Software DNV-GL Bladed. The verification of the proposed pitching system upgrade is divided into two stages. Preliminary tests for the driving motor specification is performed by Matlab analyses. The pitching motion performance is verified according to the practical WTG operation recordings (the second test stage). After the upgrade of pitch driving motors and drivers, WTGs can operate very well under serious wind conditions. In addition, once an overspeed is encountered, the blade pitch off procedure can be accomplished in time to protect the WTG after an emergency shutdown conducted. The efficacy of the upgraded system has been studied by the simulations and practical operations.

Acknowledgments

The financial support provided by Bureau of Energy (Taiwan) under the Grant 107-D0106 and Ministry of Science is gratefully acknowledged.

References

A Xia, X. Li, S. Hu, N. Li, H. Xu, “A New Pitch Control Method for Large Scale Wind Turbine Based on ADRC,” International Conference on Materials for Renewable Energy and Environment, Chengdu, China, Aug. 19-21 (2014).

A.R. Sudhamshu, C. P. Manik, S. Nivedh, N.S, Satish, M. Vivek, “Numerical Study of Effect of Pitch Angle on Performance Characteristics of A HAWT,” Engineering Science and Technology, an International Journal, 19, 632-641 (2016).

B. Biegel, M. Juelsgarrd, M. Kraning, S. Boyd, J. Stoustrup, “Wind Turbine Pitch Optimization,” IEEE International Conference on Control Applications, Sep. 28-30, Denver, CO, USA (2011).

C. Moerman, “Harakosan Technical Documentation, User’s Guide (HE-0378-R03)”, Harakosan, 2009

DNV-GL, “GH Bladed User Manual”, version 4.2, (2011).

E. Hedevang, “Wind Turbine Power Curve Incorporating Turbulence Intensity, ” Wind Energy, 17, 2, 173-195 (2014).

E. Bossanyi, A. Wright, and P. Fleming, “Further Progress with Field Testing of Individual Pitch Control,” European Wind Energy Conference, Warsaw, Poland, Apr. 20-23 (2010).

E.A. Bossanyi, “Wind Turbine Control for Load Reduction,” Wind Energy, 6, 229–244 (2003).A Xia, X. Li, S. Hu, N. Li, H. Xu, “A New Pitch Control Method for Large Scale Wind Turbine Based on ADRC,” International Conference on Materials for Renewable Energy and Environment, Chengdu, China, Aug. 19-21 (2014).

G.-B. Horizon, “Advances in Wind Power-Chapter 11: Low Speed Wind Turbine Design,” InTech, London, United Kingdom (2012).

H. Wang, R. J. Barthelmie, S. C. Pryor, H. G. Kim, “A New Turbulence Model for Offshore Wind Trubine Standards,” Wind Energy, 17, 10, 1587-1604 (2013).

Harakosan, “Hub Assembly Instructions – Turbine Type Z72”, Technical Documents and Drawings from Z72 installation (2013).

IEC, “IEC 61400-1 ed2.0, - Wind turbines - Part 1: Design requirements”, International standard of IEC publication (1999).

IEC, “IEC 61400-1-am1 ed3.0, Amendment 1 - Wind turbines - Part 1: Design requirements”, International standard of IEC publication (2010).

K. Suzuki, N. Hoshion, N. Inomata, H. Kimura, T. Fujiwara, “Influence of Wind Turbulence on Yaw-Control Gears in Wind Turbine,” Electrical Engineering in Japan, 176, 4, 15-25 (2011).

M. M. Hand, N. D. Kelley, M. J. Balas, “Identification of Wind Turbine Response to Turbulent Inflow Structure,” 4th ASME/JSME Joint Fluids Engineering Conference, Honolulu, Hawaii, Jun. 6-10 (2003).

M. Noda, R. G. J. Flay, “A Simulation Model for Wind Turbine Blade Fatigue Loads,” Journal of Wind Engineering and Industrial Aerodynamics, 83, 527-540 (1999).

N. Nanayakkara, M. Nakamura, Y. Yoshida, H. Hatazki, “Wind Turbine Control in A Small Power System at High Turbulent Wind Speeds,” IFAC Proceedings Volumes, 29, 1, 7035-7039 (1996).

P. J. Schubel, R. J. Crossley, “Wind Turbine Blade Design,” Energies, 5, 3425-3449 (2012).

R. Pedersen, S. R.K. Nielsen, P. Thoft-Christensen, P., “Stochastic Analysis of The Influence of Tower Shadow on Fatigue Life of Wind Turbine Blade,”Structural Safety, 35, 63-71 (2012).

S. Lee, M. J. Churchfield, P. J. Moriarty, J. Jonkman,

J. Michalakes, “A Numerical Study of Atmosheric and Wake Trubulence Impacts On Wind Turbine Fatigue Loadings” Journal of Solar Energy Engineering, 135 , 031001-1~031001-10 (2013).

S. Kanev and T. van Engelen, “Exploring The Limits in Individual Pitch Control, “European Wind Energy Conference, Marseille, France, Mar. 16 - 19 (2009).

S. Kanev, “Extreme Turbulence Control for Wind Turbines (ECN-E-16-062),” Energy Research Centre of The Netherlands (2016).

S. Kanev, “Extreme Turbulence Control for Wind Turbines,” Wind Engineering, 41, 5, 353-366 (2017).

Taipower Company, available at: http://www.taipower.com.tw/content/new_info/new_info-b31.aspx?LinkID=8last (accessed on 10 January 2017).

Taiwan Power Company, “Report of Renewable Energy Development in Taiwan,” 2017Blade Design,” Energies, 5, 3425-3449 (2012).

W. D. Lubitz, “Impact of Ambient Turbulence on Performance of A Small Wind Turbine,” Renewable Energy, 61, 69-73 (2014).

Y. J. Jang, C. W. Choi, J. H. Lee, K. W. Kang, “Development of Fatigue Life Prediction Method and Effect of 10-Minute Mean Wind Speed Distribution on Fatigue Life of Small Wind Turbine Composite Blade,” Renewable Energy, 78, 187-198 (2015).

Y. Yuan, J. Tang, “Adaptive Pitch Control of Wind Turbine for Load Mitigation under Structural Uncertainties,” Renewable Energy, 105, 483-494 (2017).

4C Offshore, available at: http://www.4coffshore.com/windfarms/windspeeds.aspx (accessed 15 January 2017).

NOMENCLATURE

C_p power coefficient

β twist angle of a blade

ϕ global pitch angle

α angle of attack

θ angle of relative wind

γ angle referred to the rotor position.

$F_{N,T}$ normal and tangential force of the resultant force on the blade

$F_{L,D}$ aerodynamic lift and drag force on the blade

$C_{N,T}$ coefficient of normal and tangential force

λ tip speed ratio (TSR)

w rotational speed of the rotor

r radius at the specified point

V wind velocity at blades

V_{rel} relative wind velocity

C_{pre} pressure coefficient

τ, τ_x, τ_y, τ_z induced torques to the blades in three axes

σ standard deviation of the wind speed

V_{hub} the wind velocity at the hub height

V_{ref} wind speed for defining wind turbine classes

V_{avg} average annual wind speed

I_{ref} turbulence intensity at a 10 min average wind speed of 15 m/s

Ki,w torque and voltage constant of the pitch motor

高紊流風況場址下風力機組葉片旋角系統的升級研究分析

劉瑞弘[*] 陳錦城[**] 黃金城[***] 賴文政[***]

[*]南臺科技大學機械工程系

[**]工業技術研究院 綠能與環境研究所

[***]行政院原子能委員會核能研究所

摘 要

風速風況直接影響風力機組的操作與運轉，本研究針對台灣台中風場中的 Z72-2000kW 風力機組在極端紊流風況下的運轉深入了解，發現頻繁的故障導因於控制葉片動作的旋角馬達驅動系統規格不足，致使葉片動作過慢、或是過載使得轉速超速而跳機，這也與該風場急速變化的風況有關。針對此問題，本透過軟體分析後進行了旋角驅動元件的升級，並實際進行更換，新的系統在各種劇烈風況下都能夠順利運轉，驗證本次升級的可行性。